Role of seed impurity for H-mode plasmas in JT-60U

H. Urano[1], M. Nakata[2], N. Aiba[2], H. Kubo[1], M. Honda[1], M. Yoshida[1], N. Hayashi[1], Y. Kamada[1], and the JT-60 Team[1]

[1] *Japan Atomic Energy Agency, Naka, Ibaraki 311-0193 Japan*

[2] *Japan Atomic Energy Agency, Rokkasho, Aomori 039-3212, Japan*

1 Introduction

It has been recognized that high density operation is crucial in fusion reactor from the viewpoint of sufficiently high fusion gain and mitigated heat load on the plasma facing components. However, it has also been known that energy confinement in H-modes degrades at high density. In order to avoid this problem, controlled seeding of low-Z impurity is one of the effective operations to recover the energy confinement time [1]. Recently, the energy confinement improvement with low-Z impurity seeding has been reported in metallic wall devices, such as JET [2] and ASDEX Upgrade [3]. The investigation of what role low-Z impurity plays in H-mode plasmas is an important issue in recent tokamak research. There are two main objectives of this paper which are (1) to clarify the physics picture to improve confinement with impurity seeding at high density in JT-60U and (2) to examine the role of impurity on the pedestal characteristics.

2 Experiments

The experiments were performed with and without Ar seeding in JT-60U at 1.2MA/2.5T with P_{NBI} of 17MW [1]. In a series of experiments without Ar seeding, $\bar{n}_{\mathrm{e}}$ is raised from 2.5 to $3.4\times10^{19}\mathrm{m}^{-3}$ by D_2 puff. In Ar seeded discharges, $\bar{n}_{\mathrm{e}}$ increased to $3.9\times10^{19}\mathrm{m}^{-3}$. Note that in Ar seeded case no D_2 puff was applied. This variation of $\bar{n}_{\mathrm{e}}$ was attributed to the Ar ionization. Fig. 1(a) shows the H_{H}-factor as a function of $\bar{n}_{\mathrm{e}}/n_{\mathrm{GW}}$. The H_{H}-factor decreases continuously with $\bar{n}_{\mathrm{e}}/n_{\mathrm{GW}}$ increased by D_2 puff [4]. However, better confinement at $H_{\mathrm{H}} = 0.9 - 1.0$ is sustained over the density range investigated in Ar seeded case. Fig. 1(b) and (c) indicate the impurity concentration as a function of $\bar{n}_{\mathrm{e}}$ for cases of D_2 puff and Ar puff, respectively. In unseeded case, deuterium content gradually increases with gas puff while carbon content decreases only slightly. In Ar seeded case, Ar concentration was evaluated using the charge neutrality and the definition of Z_{eff}, where Z_{eff} and the carbon concentration were measured

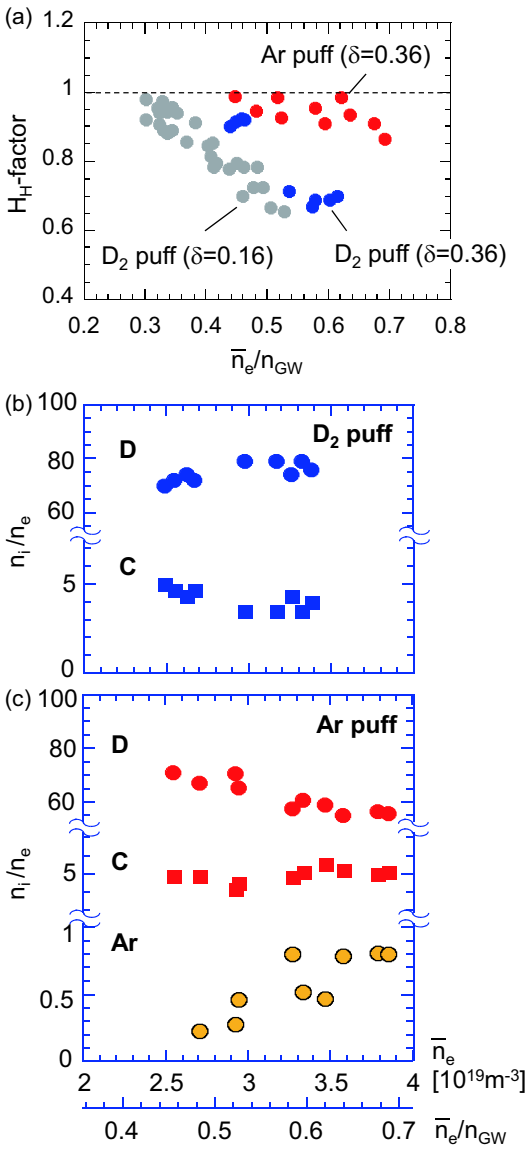

FIG. 1: (a) The H_{H} factor as a function of $\bar{n}_{\mathrm{e}}/n_{\mathrm{GW}}$. Impurity concentration fractions as a function of line-averaged electron density in cases of (b) D_2 puff and (c) Ar puff.

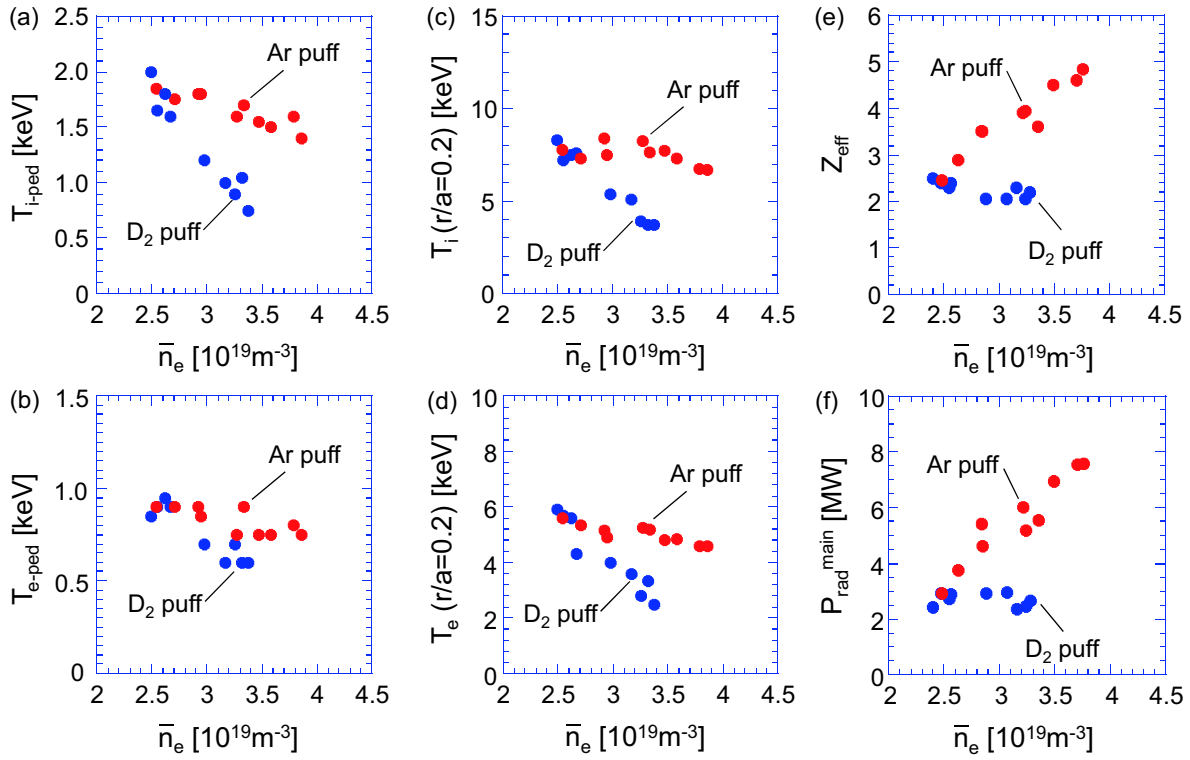

FIG. 2: The variations of (a) $T_{\mathrm{i-ped}}$, (b) $T_{\mathrm{e-ped}}$, (c) T_{i} at $r/a = 0.2$, (d) T_{e} at $r/a = 0.2$, (e) Z_{eff} and (f) $P_{\mathrm{rad}}^{\mathrm{main}}$as a function of $\bar{n}_{\mathrm{e}}$ for cases with and without Ar seeding.

with visible Bremsstrahlung and charge-exchange recombination spectroscopy (CXRS), respectively. Since the electrons are supplied with Ar ionization, the increase of $\bar{n}_{\mathrm{e}}$ corresponds to the increase of Ar concentration from 0.2% to 0.8%. Deuterium content decreases continuously with the increase of Ar concentration while carbon content remains nearly constant. At $\bar{n}_{\mathrm{e}}/n_{\mathrm{GW}}$ of 0.6, dilution is enhanced by $\sim 15\%$ from the case without Ar.

3 Energy confinement with Ar seeded H-mode plasmas

Figs. 2(a)-(d) plot the values of $T_{\mathrm{i-ped}}$, $T_{\mathrm{e-ped}}$, T_{i} at $r/a = 0.2$, and T_{e} at $r/a = 0.2$ as a function of $\bar{n}_{\mathrm{e}}$, respectively. In D_2 puffed case, both the pedestal and core T_{i} decrease continuously with increasing $\bar{n}_{\mathrm{e}}$. However, in Ar seeded case, the reduction in the pedestal and core T_{i} due to an increase in density weakens in comparison with the case without Ar seeding. The similar behavior is also seen in the electron temperatures. Figs. 2(e) and (f) shows the variarion of Z_{eff} and $P_{\mathrm{rad}}^{\mathrm{main}}$ with $\bar{n}_{\mathrm{e}}$, respectively. As the density is raised with Ar seeding rate, Z_{eff} increases from 2.4 to 5.0, whereas it decreases slightly from 2.5 to 2.0 by D_2 puff. The $P_{\mathrm{rad}}^{\mathrm{main}}$ also increases with Ar concentration from 3MW to 8MW, whereas it does not change largely for D_2 puff case.

Fig. 3(a) shows a pair of n_{e} profiles for cases with D_2 puff and Ar puff (0.8%) at a given $\bar{n}_{\mathrm{e}}/n_{\mathrm{GW}}$ of 0.58. The n_{e} profiles tend to be flatter with increased D_2 puff rate, whereas peaked density profiles are kept at high density in Ar seeded discharges. When a pair of plasmas at a given averaged density ($\bar{n}_{\mathrm{e}}/n_{\mathrm{GW}} = 0.58$) are chosen, the n_{e} profile is more peaked with Ar seeding than with D_2 puff, which leads to relatively lower edge density. Fig. 3(b) shows a pair of T_{i} profiles for cases with D_2 puff and Ar puff (0.8%) at a given $\bar{n}_{\mathrm{e}}/n_{\mathrm{GW}}$ of 0.58. At a given averaged density, higher T_{i} is obtained over the entire range of minor radius for the

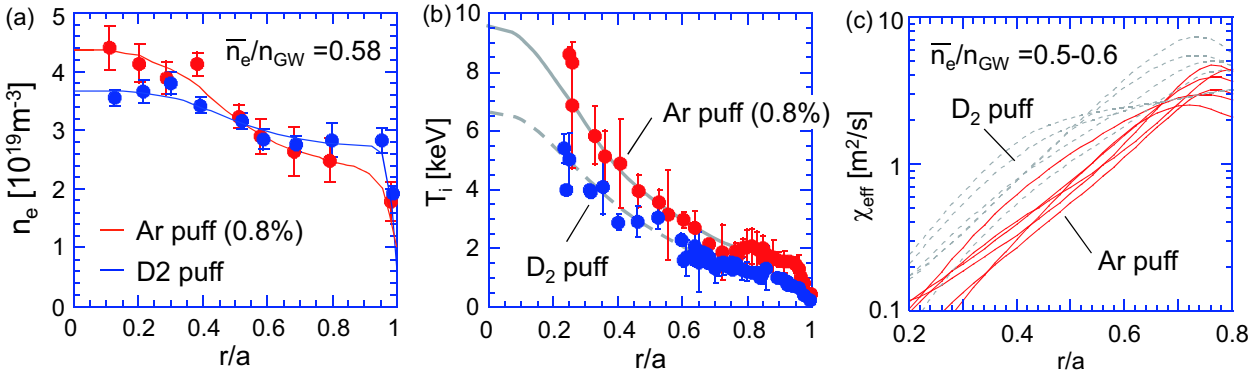

FIG. 3: Spatial profiles of (a) n_e and (b) T_i for cases with D_2 puff and Ar puff (0.8%) at a given $\bar{n}_e/n_{GW}$ of 0.58. (c) The χ_{eff} profiles for cases with and without Ar puff in the range of $\bar{n}_e/n_{GW} = 0.5 - 0.6$.

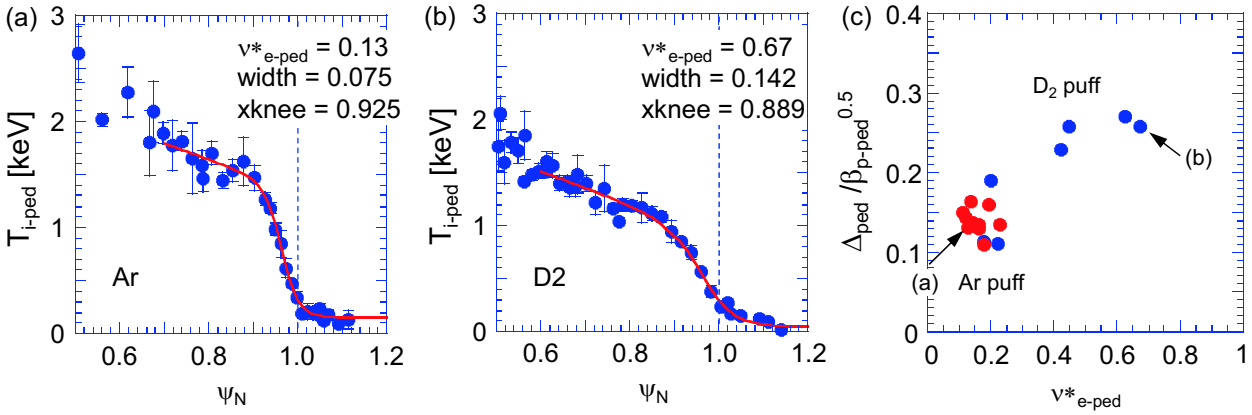

FIG. 4: Spatial profiles of T_i for cases with (a) Ar puff at low ν^*_{e-ped} of 0.13 and (b) D_2 puff at high ν^*_{e-ped} of 0.67. (c) The pedestal width normalized to $\beta^{0.5}_{p-ped}$ as a function of ν^*_{e-ped}.

case with Ar seeding. Fig. 3(c) shows the χ_{eff} profiles for cases with and without Ar puff in the range of $\bar{n}_e/n_{GW} = 0.5 - 0.6$. The values of χ_{eff} are lower systematically with Ar seeding than with D_2 puff case in the core plasma region.

An increase of pedestal density with D_2 puff leads to a reduction of pedestal temperature so that the pedestal pressure remains nearly constant at $0.7 - 0.8$kPa. In case of Ar seeding, the pedestal pressure also remains nearly constant at $0.7 - 0.8$kPa in the variation of Ar puff. However, Higher pedestal temperature is sustained in case with Ar puff accompanied by lower n_{e-ped} and n_{i-ped}. There are two reasons for reducing n_{e-ped} and n_{i-ped} with Ar puff. One is that n_{e-ped} becomes lower with Ar seeding due to peaking effect. This difference becomes larger at high density because density profiles become flatter in conventional H-modes. The other is that reduction in n_{i-ped} is larger approximately by a factor of two with Ar puff than that in n_{e-ped}. This reduction is composed by peaking effect and dilution effect at nearly the same fraction.

4 Edge pedestal characteristics

Dependence of pedestal width on ρ^*_p and β_p has intensively been studied in many tokamaks. However, dependence of pedestal width on ν^*_e and configuration parameters, such as δ, κ, ϵ, has not been investigated. In this series of experiment, β_p remains nearly constant at ~ 0.3 whereas ν^*_e varies widely from 0.2 to 0.7. Figs. 4(a) and (b) show the edge T_i profiles with Ar puff at low ν^*_{e-ped} of 0.13 and D_2 puff at high ν^*_{e-ped} of 0.67, respectively.

The pedestal width with Ar puff at low ν_e^* is clearly narrower than that with D_2 puff at high ν_e^*. Fig. 4(c) shows the pedestal width normalized to $\beta_{p-ped}^{0.5}$ [5] as a function of ν_{e-ped}^*. Pedestal width becomes larger with increased ν_e^* despite β_p being kept nearly constant. On the other hand, pedestal width does not change clearly in Ar seeded case. The ν_e^* remains nearly constant at $\sim$ 0.2 in Ar seeded case. One can find that pedestal width increases with ν_e^* consistently whether or not Ar is seeded.

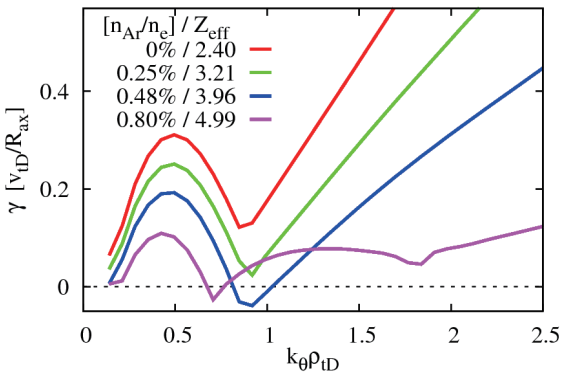

FIG. 5: Linear ITG-TEM mode spectra in the variation of Ar concentration calculated by GKV code.

5 Discussion and conclusions

Dependence of transport levels and of the strength of profile stiffness on impurity concentration is also a challenging issue. Fig. 5 shows the wavenumber spectra of ITG-TEM mode growth rate in the variation of Ar concentration calculated by a local gyrokinetic code (GKV) [6]. We found a stabilization due to ion dilution and increasing Z_{eff} on ITG-TEM mode, which is qualitatively consistent with experimental tendency of heat transport levels shown in Fig. 3(c). On the other hand, the quasi-linear estimates on particle flux seem to be not sufficient against the experimental results. The neoclassical and/or turbulence pinch effects should be examined as the next step study.

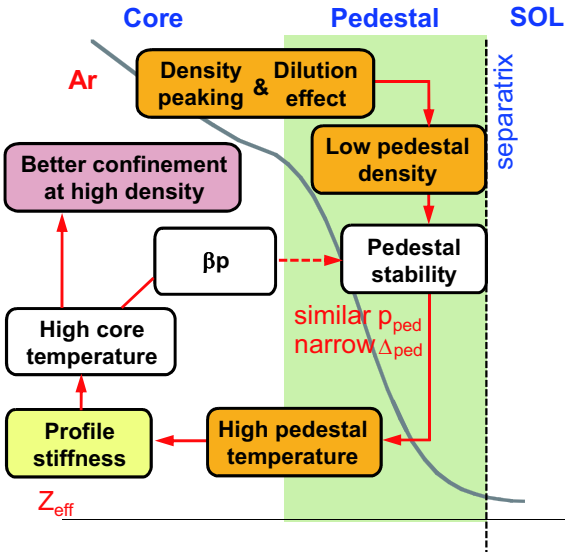

FIG. 6: Schematic view of pressure profile in H-mode plasmas explaining the physics picture of how Ar seeding improves energy confinement.

Physics picture to improve confinement with Ar seeding at high density has been investigated in JT-60U. Fig. 6 shows the schematic view of pressure profile in H-mode plasmas. Better confinement was sustained at high density by Ar seeding accompanied by higher core and pedestal temperatures. Density profiles became flatter with D_2 puff in conventional H-mode plasmas, whereas peaked density profiles were kept with Ar seeding. Pedestal pressure remains constant where reduction in pedestal density with Ar puff is due to density peaking and dilution effect. Higher $T_{e,i-ped}$ gives a boundary condition for high core temperature and thus better confinement is obtained with Ar seeding.

References

[1] Kubo, H., et al., Nucl. Fusion **41** (2001) 227.
[2] Matthews, G., et al., Physica Scripta **T128** (2007) 137.
[3] Neu, R., et al., J. Nucl. Meter. **438** (2013) S34.
[4] Urano, H., et al., Nucl. Fusion **42** (2002) 76.
[5] Urano, H., et al., Nucl. Fusion **48** (2008) 045008.
[6] Nakata, M., et al., Plasma and Fusion Res. **9** (2014) 1403029.